

UC Irvine

UC Irvine Previously Published Works

Title

Anandamide suppresses pain initiation through a peripheral endocannabinoid mechanism

Permalink

<https://escholarship.org/uc/item/71w3n0qd>

Journal

Nature Neuroscience, 13(10)

ISSN

1097-6256

Authors

Clapper, Jason R
Moreno-Sanz, Guillermo
Russo, Roberto
et al.

Publication Date

2010-10-01

DOI

10.1038/nn.2632

Copyright Information

This work is made available under the terms of a Creative Commons Attribution License, available at <https://creativecommons.org/licenses/by/4.0/>

Peer reviewed



Published in final edited form as:

Nat Neurosci. 2010 October ; 13(10): 1265–1270. doi:10.1038/nn.2632.

Anandamide suppresses pain initiation through a peripheral endocannabinoid mechanism

Jason R. Clapper^{1,*}, Guillermo Moreno-Sanz^{1,2,*}, Roberto Russo^{3,*}, Ana Guijarro¹, Federica Vacondio⁴, Andrea Duranti⁵, Andrea Tontini⁵, Silvano Sanchini⁵, Natale R. Sciolino⁶, Jessica M. Spradley⁶, Andrea Hohmann^{6,7}, Antonio Calignano³, Marco Mor⁴, Giorgio Tarzia⁵, and Daniele Piomelli^{1,8,#}

¹Department of Pharmacology, University of California, Irvine, 360 MSRII, Irvine, CA, 92697, USA

²Department of Biochemistry and Molecular Biology III, Complutense University, Ciudad Universitaria, Madrid, Spain 28040

³Department of Experimental Pharmacology, University of Naples “Federico II”, via D. Montesano 49, Naples, Italy 80131

⁴Pharmaceutical Department, University of Parma, viale G.P. Usberti 27/A, Campus Universitario, Parma, Italy 43100

⁵Department of Health and Drug Sciences, University of Urbino “Carlo Bo”, Piazza Rinascimento, 6, Urbino, Italy 61029

⁶Neuroscience and Behavior Program, Department of Psychology, University of Georgia, Athens, GA, 30602-3013, USA

⁷Program in Neuroscience, Biomedical Health Science Institute, University of Georgia, Athens, GA, 30602-3013, USA

⁸Drug Discovery and Development, Italian Institute of Technology, via Morego 30, Genoa, Italy 16163

Abstract

Peripheral cannabinoid receptors exert a powerful inhibitory control over pain initiation, but the endocannabinoid signal that normally engages this intrinsic analgesic mechanism is unknown. To address this question, we developed a peripherally restricted inhibitor of fatty acid amide hydrolase (FAAH), the enzyme responsible for the degradation of the endocannabinoid anandamide. The compound, called URB937, suppresses FAAH activity and increases anandamide levels outside the central nervous system (CNS). Despite its inability to access brain and spinal cord, URB937 attenuates behavioral responses indicative of persistent pain in rodent models of peripheral nerve injury and inflammation, and prevents noxious stimulus-evoked neuronal activation in spinal cord regions implicated in nociceptive processing. CB₁ cannabinoid receptor blockade prevents these effects. The results suggest that anandamide-mediated signaling at peripheral CB₁ receptors controls the access of pain-related inputs to the CNS. Brain-impenetrant FAAH inhibitors, which strengthen this gating mechanism, might offer a new approach to pain therapy.

#Corresponding author: Daniele Piomelli, PhD, Italian Institute of Technology, Department of Drug Discovery and Development, via Morego 30, Genoa, Italy 16163, Phone: (39) 010-71781442, Fax: (39) 010-7170187, daniele.piomelli@iit.it or piomelli@uci.edu.

*Equal contributions.

Conflict of interest

We wish to acknowledge a conflict of interest. A patent covering URB937 and allied compounds has been filed on behalf of the inventors by the University of California, Irvine, the Italian Institute of Technology, and the Universities of Urbino and Parma.

Introduction

Pain perception can be effectively controlled by neurotransmitters that operate within the CNS. This modulation has been well characterized in the dorsal horn of the spinal cord, where impulses carried by nociceptive (pain-sensing) fibers are processed before they are transmitted to the brain. In addition to these central mechanisms, intrinsic control of pain transmission can occur at terminals of afferent nerve fibers outside the CNS. One prominent example of peripheral regulation is provided by the endogenous opioids, which are released from activated immune cells during inflammation and inhibit pain initiation by interacting with opioid receptors localized on sensory nerve endings^{1,2}.

Endocannabinoid mediators might serve an analogous function to that of the opioids, because pharmacological activation of peripheral CB₁ and CB₂ cannabinoid receptors inhibits pain-related behaviors^{3–7} while genetic disruption of CB₁ receptor expression in primary nociceptive neurons exacerbates such behaviors⁸. Moreover, there is evidence that clinical conditions associated with neuropathic pain or inflammation are accompanied by peripheral elevations in the levels of the endocannabinoid anandamide (e.g., complex regional pain syndrome and arthritis)^{9,10}. Another major endocannabinoid transmitter, 2-arachidonoylglycerol (2-AG), has also been implicated in nociceptive signaling outside the CNS^{8,11}.

Although these findings suggest that the endocannabinoid system serves an important function in the peripheral regulation of nociception, they offer no definitive insight on the identity of the endogenous ligand, or ligands, involved in this function. Filling this gap is essential, however, to both define the molecular underpinnings of intrinsic mechanisms controlling pain initiation and to discover new analgesic agents devoid of unwanted central effects. In the present study, we describe a potent brain-impenetrant inhibitor of the anandamide-degrading enzyme FAAH, and use this drug to magnify the actions of peripheral anandamide and unmask its possible role in the control of pain initiation¹².

Results

Discovery of a peripherally restricted FAAH inhibitor

Current FAAH inhibitors readily cross the blood-brain barrier¹². To produce inhibitors with restricted access to the CNS, we added chemical groups of varying polarity to the proximal phenyl ring of the brain-permeant *O*-arylcarbamate URB597^{13,14} (Table 1, **1a**), in a position where small-sized hydrophilic substituents are not expected to impair biological activity¹⁵. The new compounds had comparable potencies when tested in membrane preparations of rat brain FAAH, and were equally effective at blocking liver FAAH activity when administered systemically in mice (1 mg·kg⁻¹, intraperitoneal, i.p.) (Table 1, compounds **1b–1f**). They markedly differed, however, in their ability to access the CNS. In particular, the *p*-hydroxyphenyl derivative URB937 (Table 1, **1b**) suppressed FAAH activity in peripheral tissues of mice and rats, yet failed to affect FAAH activity in the brain (Table 1, Supplementary Table 1). A dose-exploration study in mice showed that the median effective dose (ED₅₀) of URB937 for FAAH inhibition in brain (40 mg·kg⁻¹, subcutaneous, s.c.) was 200 times higher than the ED₅₀ for FAAH inhibition in liver (0.2 mg·kg⁻¹, s.c.) (Fig. 1a). Moreover, after systemic administration, URB937 (1 mg·kg⁻¹, i.p.) distributed rapidly in blood and liver, but remained undetectable in brain tissue (Fig. 1b). As seen with other *O*-arylcarbamates, which are known to interact with FAAH through a covalent mechanism^{13,16}, URB937 inhibited peripheral FAAH activity *in vivo* both rapidly and lastingly (Supplementary Figure 1).

Mechanism of peripheral segregation

Because of its lipophilicity, URB937 should passively diffuse into the CNS unless this diffusion process is actively countered (distribution coefficient, $\text{LogD}_{\text{oct,pH7.4}}$: URB937, 3.03 ± 0.01 ; CNS-penetrant inhibitor, URB597, 3.71 ± 0.01 ; $\text{mean} \pm \text{s.e.m.}$, $n = 3$). To test these alternative possibilities, we determined the permeability and efflux ratios of URB937 through polarized monolayers of human epithelial TC7 cells, which express various protein transporters involved in the extrusion of drugs from the brain¹⁷. URB937 did not equally distribute across the apical (A) and basal (B) compartments of TC7 monolayers, as would be expected of a lipophilic molecule moving by passive diffusion. Rather, the compound accumulated into the A compartment [permeability, in $\text{nm}\cdot\text{s}^{-1}$ (% recovery) A–B, 38 (83%); B–A, 371 (95%); efflux ratio, 9.8; mean of 2 independent experiments]. This result suggests that URB937 might be extruded from the CNS. Supporting this interpretation, injection of URB937 into the lateral cerebral ventricles of rats ($0.01\text{--}0.1 \text{ mg}\cdot\text{kg}^{-1}$) was followed by appearance of the compound in peripheral blood (Fig. 1c) and concurrent inhibition of FAAH activity in liver (Fig. 1d). Conversely, systemic administration of a 250 times higher dose of URB937 ($25 \text{ mg}\cdot\text{kg}^{-1}$, i.p.) had no effect on brain FAAH activity (Fig. 1e), which was markedly reduced by a low dose of the CNS-penetrant inhibitor URB597 ($1 \text{ mg}\cdot\text{kg}^{-1}$, i.p.) (Fig. 1e).

To gain insight into the transport mechanism involved in the extrusion of URB937 from the CNS, we administered various inhibitors of drug transport across the blood-brain barrier, together with a systemic dose of URB937 that did not achieve brain penetration ($25 \text{ mg}\cdot\text{kg}^{-1}$, i.p.). Treatment with Ko-143 ($10 \text{ mg}\cdot\text{kg}^{-1}$, i.p.) – an inhibitor of the ATP-binding cassette transporter, breast cancer resistance protein (BCRP)¹⁷ – markedly increased access of URB937 to the brain (Fig. 1e). A similar effect was obtained with 2,6-dichloro-4-nitrophenol¹⁸, which blocks the sulfate conjugation required for BCRP-mediated transport of xenobiotics¹⁹ (Fig. 1e). By contrast, administration of other drug-transport inhibitors – including verapamil, probenecid and rifampicin¹⁷ – was ineffective (Fig. 1e). The results suggest that URB937 is exported from the CNS by a transport system that is pharmacologically indistinguishable from BCRP. The molecular identification of such system will require, however, additional experimentation.

Enhancement of peripheral anandamide signaling

Administration of URB937 ($1 \text{ mg}\cdot\text{kg}^{-1}$, i.p.) in mice increased anandamide levels in peripheral tissues, but not forebrain or hypothalamus (Fig. 1f, Supplementary Figure 2a). This effect was caused by selective inhibition of FAAH activity because (i) it was accompanied by elevations of other FAAH substrates, such as palmitoylethanolamide (PEA)²⁰ (Fig. 1f); and (ii) it was not observed in mutant FAAH-deficient mice²¹ (Fig. 1g). Importantly, URB937 did not affect monoacylglycerol lipase activity *in vitro* (median inhibitory concentration, IC_{50} , $>100 \mu\text{M}$; $n = 3$) or alter tissue levels of its endocannabinoid substrate, 2-AG, *in vivo* (Supplementary Figure 2b).

Modulation of visceral pain

Current FAAH inhibitors attenuate behavioral responses to noxious stimuli in rodents, a property that is generally attributed to their ability to augment anandamide signaling in brain and spinal cord^{12,13}. To test whether peripheral anandamide contributes to these actions, we examined the effects of URB937 on nocifensive responses evoked by acetic acid injection into the peritoneal cavity of mice. Subcutaneous administration of URB937 reduced acetic acid-induced writhing with an ED_{50} of $0.1 \text{ mg}\cdot\text{kg}^{-1}$ (Fig. 2a and data not shown). This effect was (i) comparable in efficacy to those elicited by CNS-penetrant FAAH inhibitor URB597 and cyclooxygenase inhibitor indomethacin (each at $1 \text{ mg}\cdot\text{kg}^{-1}$, s.c.) (Fig. 2a); (ii) correlated with the degree of peripheral FAAH inhibition (Pearson correlation coefficient, r

= 0.96, Fig. 2b); and (iii) absent in mutant FAAH-deficient mice, compared to their wild-type littermates (Fig. 2c). The antinociceptive effect of URB937 was blocked by the selective CB₁ antagonists rimonabant and AM251, but not by the CB₂ antagonist AM630 (each at 1 mg·kg⁻¹, s.c.) (Fig. 2d). Although anandamide can activate vanilloid type-1 transient receptor potential (TRPV-1) channels²², URB937 evoked no detectable nocifensive behavior when administered alone (Fig. 2a), which suggests that the tissue concentrations reached by endogenous anandamide following peripheral FAAH inhibition are insufficient to engage TRPV-1 channels.

Treatment with URB937 elevated tissue levels of PEA (Fig. 1f), an endogenous peroxisome proliferator-activated receptor- α (PPAR- α) agonist that acts synergistically with anandamide to attenuate pain responses in rodents^{3,23,24}. Co-administration of PPAR- α antagonist MK-886 (1 mg·kg⁻¹, s.c.) or genetic disruption of PPAR- α prevented the effects of URB937 in mice (Fig. 2d,e). We interpret these findings to indicate that URB937 inhibits acetic acid-induced pain responses through a mechanism that requires both anandamide-dependent activation of CB₁ receptors and PEA-dependent activation of PPAR- α .

Modulation of neuropathic and inflammatory pain

We next asked whether URB937 might influence persistent pain caused by nerve damage or inflammation. We produced peripheral nerve injury in mice by loosely tying the left sciatic nerve²⁵. A single dose of URB937 (1 mg·kg⁻¹, i.p., 2 h before testing), administered one week after surgery, attenuated thermal hyperalgesia and suppressed mechanical hyperalgesia and mechanical allodynia on the operated side (Fig. 3a–c). Notably, this response was not accompanied by changes in the reactivity to cutaneous stimuli applied to the non-operated side, indicating that URB937 normalized mechanical and thermal thresholds altered by nerve injury, rather than exerting a generalized antinociceptive action (Fig. 3a–c). This conclusion was further supported by the lack of activity of URB937 in the hot-plate test (Supplementary Figure 3). As previously shown for URB597²⁶, subchronic treatment with URB937 (1 mg·kg⁻¹, i.p.) once daily for 7 days, starting 3 days after nerve ligation, elicited a set of analgesic effects that were indistinguishable from those caused by single drug dosing (Fig. 3d–f). Moreover, such effects were completely blocked by rimonabant, but not by AM630 (Fig. 3g–i) or MK886 (each at 1 mg·kg⁻¹, s.c.) (Supplementary Figure 4).

In another group of mice, we induced peripheral inflammation by injecting the polysaccharide carrageenan into one of the hind paws. This resulted in the development of mechanical and thermal hyperalgesia as well as local edema (Fig. 4). A single systemic injection of URB937 (1 mg·kg⁻¹, i.p.), administered at the same time as carrageenan, decreased mechanical and thermal hyperalgesia, assessed 4 h and 24 h following carrageenan treatment (Fig. 4a,b). URB937 also reduced mechanical allodynia measured 24 h after carrageenan (Fig. 4c). Similar results were obtained when treating mice with the CNS-permeant inhibitor URB597 (1 mg·kg⁻¹, i.p.) (Supplementary Figure 5). The antihyperalgesic effects of URB937 were restricted to the inflamed paws (Supplementary Figure 6) and were prevented by rimonabant, but not by AM630 (Fig. 4a–c) or MK886 (Supplementary Figure 7) (each at 1 mg·kg⁻¹, i.p.). Moreover, URB937 reversed paw edema 24 h after carrageenan injection through a mechanism that was sensitive to both CB₁ and CB₂ receptor blockade (Fig. 4d). Subchronic treatment with URB937 (1 mg·kg⁻¹, i.p., once daily for 3 days) was effective at inhibiting carrageenan-induced pain and edema (Supplementary Figure 8). Together, the results indicate that URB937 alleviates neuropathic and inflammatory pain in mice through a mechanism that primarily depends on the activation of peripheral CB₁ receptors by endogenously produced anandamide.

Modulation of spinal nociceptive processing

To determine whether URB937 alters the central processing of nociceptive inputs, we measured spinal cord expression of Fos protein, a marker of neuronal activity, in a model of persistent pain produced by administration of formalin into the dorsal hind paw of rats. Formalin elicited a marked nocifensive response, which was attenuated by co-injection of URB937 (1 mg·kg⁻¹, i.p.). The drug reduced formalin-induced pain behavior relative to vehicle, the CB₁ antagonist rimonabant (2 mg·kg⁻¹, i.p.), or a combination of rimonabant and URB937 (Fig. 5a). Further analyses revealed that (i) URB937 decreased the area under the curve of formalin-induced pain behavior, compared to all other treatment groups (Supplementary Figure 9a); and (ii) this effect was due to a reduction in the late phase (Phase 2) of the formalin response (Fig. 5b, Supplementary Figure 9b), during which ongoing primary afferent fiber activity is accompanied by inflammation and central sensitization of spinal nociceptive circuits^{27,28}.

URB937 lowered the Fos response to formalin in spinal cord regions implicated in nociceptive processing (Fig. 5c–e), namely the superficial (lamina I,II) and neck regions of the dorsal horn (lamina V, VI) (Fig. 5f). To a lesser extent, URB937 also suppressed Fos protein expression in the *nucleus proprius* (lamina III, IV) and ventral horn (Fig. 5f). These effects were prevented by the CB₁ antagonist rimonabant (2 mg·kg⁻¹, i.p.), which did not significantly alter Fos levels when administered without URB937 (Fig. 5f). The ability of URB937 to modulate spinal nociceptive processing, despite its lack of CNS penetration, suggests that peripheral FAAH inhibition attenuates pain-related inputs before they enter the spinal cord.

Effects on food intake and spontaneous locomotion

Cannabinoid receptor agonists stimulate feeding through both central and peripheral mechanisms²⁹. As previously shown for the CNS-penetrant FAAH inhibitor URB597¹⁴, administration of URB937 (1 mg·kg⁻¹, i.p., 30 min before dark) did not alter daily food intake, feeding pattern (latency to feed, meal frequency, satiety ratio) or spontaneous locomotor activity in mice (Supplementary Figure 10).

Discussion

The compound URB937, which we disclose in the present study, is a potent FAAH inhibitor that does not readily enter the CNS and thus interrupts anandamide deactivation only in peripheral tissues. Despite this restricted range of action, URB937 causes marked antinociceptive effects in rodent models of acute and persistent pain, which are prevented by cannabinoid CB₁ receptor blockade. These findings suggest that inhibition of peripheral FAAH activity magnifies an endogenous analgesic mechanism, mediated by anandamide, which regulates the transmission of emerging pain signals to the spinal cord and the brain.

We hypothesize that peripheral anandamide acts as a diffuse paracrine signal to modulate the intensity of pain stimuli as they arise in damaged tissues. Two lines of evidence support this idea. Firstly, signals generated by inflammation and neural injury can trigger the local production and release of anandamide. For example, membrane depolarization and activation of TRPV-1 channels each stimulates anandamide formation in cultures of sensory neurons³⁰, while activation of Toll-like receptor 4 causes a similar effect in macrophages³¹. These signals, and likely others that remain to be identified, may contribute to the elevations in peripheral anandamide documented in animal models of spinal nerve injury and inflammation^{8,11} as well as in painful human conditions such as complex regional pain syndrome⁹ and arthritis¹⁰. Secondly, CB₁ receptors are broadly distributed throughout mammalian tissues and organs. In particular, they are expressed in primary sensory neurons

of heterogeneous sizes and are transported to peripheral nerve endings^{32,33}. There, CB₁ receptor activation may be both necessary to maintain normal pain thresholds⁸ and sufficient to exert marked antinociceptive effects^{3,6}. CB₁ receptors present on pain-sensing terminals may mediate the analgesic and anti-inflammatory actions of locally produced anandamide through their inhibitory influence on the release of excitatory neuropeptides³⁴. Other receptors are likely to contribute, along with CB₁, to anandamide signaling in response to injury. Two candidates are CB₂ and PPAR- α , which are present in immune cells and peripheral sensory neurons, and act synergistically with CB₁ to reduce pain^{3,23,24,35,36}. Our results suggest, indeed, that CB₁ receptors cooperate both with PPAR- α , to modulate visceral pain in the acetic acid model, and with CB₂, to reduce edema in the carrageenan model. Importantly, however, CB₁ receptors appear to play an exclusive role in mediating the analgesic effects of URB937 in models of neuropathic and inflammatory pain.

Mutant mice in which FAAH expression is selectively disrupted in non-neuronal cells, but is preserved in peripheral and central neurons, display a striking phenotype in which normal nociceptive transmission is accompanied by reduced responsiveness to pro-inflammatory triggers³⁷. A plausible explanation for this finding is that the signaling activity of anandamide at peripheral nociceptive neurons is influenced by FAAH localized to the nociceptors themselves, rather than to neighboring non-neural cells. This view is consistent with the observation that peripheral axotomy induces FAAH expression in large-sized sensory neurons of the dorsal root ganglia, a response that is expected to extend the colocalization of FAAH with CB₁ receptors and thus enhance the ability of this enzyme to terminate anandamide signaling³⁸.

Direct activation of peripheral cannabinoid receptors causes profound analgesic effects in experimental models of pain^{2,39}. Our findings indicate that significant analgesia can also be obtained by magnifying the intrinsic activity of an anandamide-based signaling system involved in the dynamic regulation of nociceptive homeostasis outside the CNS. These findings offer new insights into the intrinsic control of pain and might be exploited therapeutically to develop analgesic agents devoid of central side effects.

Materials and Methods

Synthesis of FAAH inhibitors

A description of the synthetic procedures is found in the Supplementary Methods section.

Drug distribution coefficients

We determined Log *D* values at room temperature (25±1°C) partitioning the solutes between *n*-octanol and an aqueous solution buffered at pH 7.4⁴⁰.

Enzyme assays

We conducted standard FAAH and monoacylglycerol lipase assays as described^{15,41}, using as substrates [³H]-anandamide (American Radiolabeled Chemicals, Inc., St. Louis, MO) and 2-oleoyl-*sn*-glycerol (Nu-Check Prep, Elysian, MN), respectively.

Drug transport assays

Assays were performed at Cerep Inc. (Redmond, WA), following protocols outlined in the Supplementary Methods section.

Tissue analyses

We performed tissue extractions and liquid chromatography/mass spectrometry analyses of endocannabinoids as described⁴². Procedures for tissue extraction and quantification of URB937 are detailed in Supplementary Methods.

Surgery

We performed sciatic nerve ligations in male Swiss Webster mice, as previously described for rats²⁵ with minor modifications²⁶. Cannula implantation for i.c.v. infusions is described in Supplementary Methods.

Behavioral tests

We measured nocifensive responses elicited by i.p. injection of acetic acid in male Swiss Webster and C57Bl/6 (wild-type, FAAH-deficient, PPAR- α -deficient) mice⁴³, intraplantar injection of carrageenan in male Swiss Webster mice²⁰, intraplantar injection of formalin in male Sprague-Dawley rats⁴⁴, and sciatic nerve ligation in male Swiss Webster mice²⁶.

Fos expression

We measured Fos protein levels by quantitative immunocytochemistry⁵ on slices of lumbar (L4/L5) spinal cord from the same rats used for the formalin test.

Supplementary Material

Refer to Web version on PubMed Central for supplementary material.

Acknowledgments

We thank Emmanuel Dotsey for help with experiments. This research was supported by grants from the National Institutes on Drug Abuse (to D.P. and A.G.H.), the University of Parma (to M.M.), and the Italian Ministry for Public Education, University and Research (MIUR) (to G.T. A.D and A.T.). Guillermo Moreno-Sanz was partially supported by the Fulbright Commission and the Exchange Abroad Program, University of California. The support of the Agilent Foundation is gratefully acknowledged.

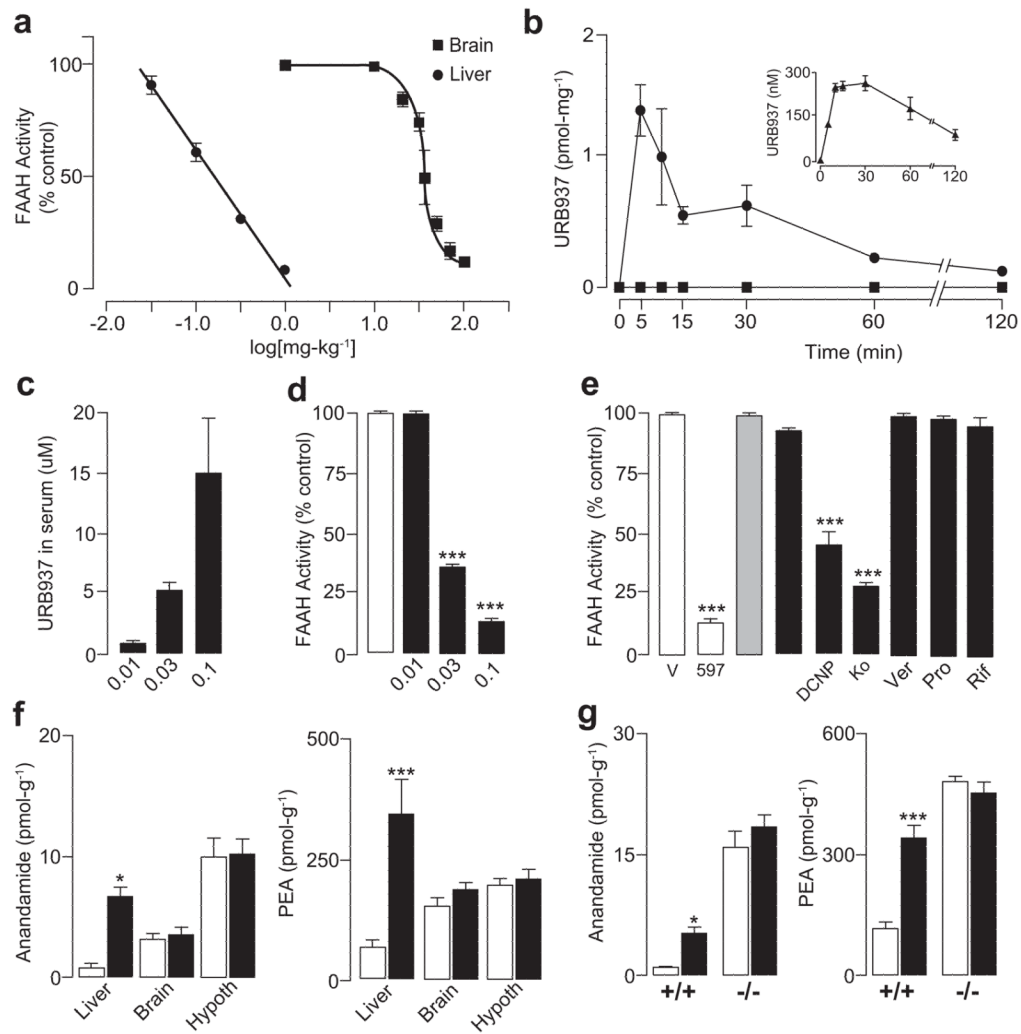
References

1. Stein C, Schafer M, Machelska H. Attacking pain at its source: new perspectives on opioids. *Nat Med.* 2003; 9 (8):1003–1008. [PubMed: 12894165]
2. Stein C, Zollner C. Opioids and sensory nerves. *Handb Exp Pharmacol.* 2009; (194):495–518. [PubMed: 19655116]
3. Calignano A, La Rana G, Giuffrida A, Piomelli D. Control of pain initiation by endogenous cannabinoids. *Nature.* 1998; 394 (6690):277–281. [PubMed: 9685157]
4. Jaggar SI, Sellaturay S, Rice AS. The endogenous cannabinoid anandamide, but not the CB2 ligand palmitoylethanolamide, prevents the viscerovisceral hyper-reflexia associated with inflammation of the rat urinary bladder. *Neurosci Lett.* 1998; 253 (2):123–126. [PubMed: 9774165]
5. Nackley AG, Suplita RL 2nd, Hohmann AG. A peripheral cannabinoid mechanism suppresses spinal fos protein expression pain behavior in a rat model of inflammation. *Neuroscience.* 2003; 117 (3):659–670. [PubMed: 12617970]
6. Dziadulewicz EK, et al. Naphthalen-1-yl-(4-pentyloxynaphthalen-1-yl)methanone: a potent, orally bioavailable human CB1/CB2 dual agonist with antihyperalgesic properties and restricted central nervous system penetration. *J Med Chem.* 2007; 50 (16):3851–3856. [PubMed: 17630726]
7. Anand P, Whiteside G, Fowler CJ, Hohmann AG. Targeting CB2 receptors and the endocannabinoid system for the treatment of pain. *Brain Res Rev.* 2009; 60 (1):255–266. [PubMed: 19150370]

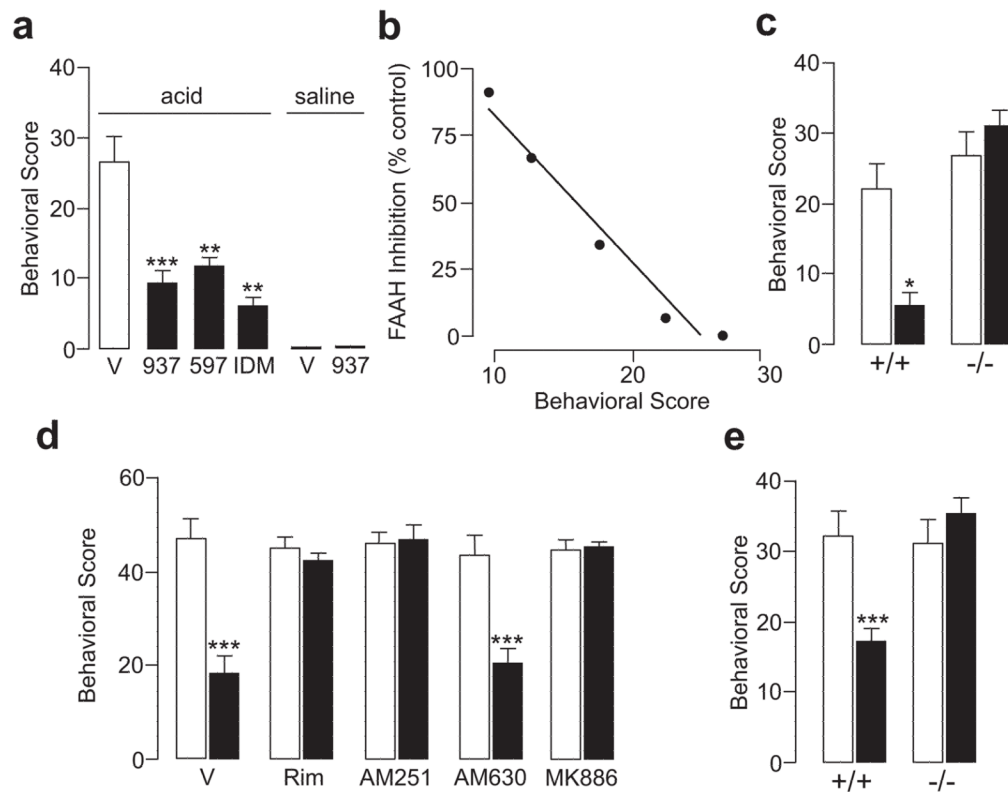
8. Agarwal N, et al. Cannabinoids mediate analgesia largely via peripheral type 1 cannabinoid receptors in nociceptors. *Nat Neurosci.* 2007; 10 (7):870–879. [PubMed: 17558404]
9. Kaufmann I, et al. Enhanced anandamide plasma levels in patients with complex regional pain syndrome following traumatic injury: a preliminary report. *Eur Surg Res.* 2009; 43 (4):325–329. [PubMed: 19729930]
10. Richardson D, et al. Characterisation of the cannabinoid receptor system in synovial tissue and fluid in patients with osteoarthritis and rheumatoid arthritis. *Arthritis Res Ther.* 2008; 10 (2):R43. [PubMed: 18416822]
11. Mitrirattanakul S, et al. Site-specific increases in peripheral cannabinoid receptors and their endogenous ligands in a model of neuropathic pain. *Pain.* 2006; 126 (1–3):102–114. [PubMed: 16844297]
12. Schlosburg JE, Kinsey SG, Lichtman AH. Targeting fatty acid amide hydrolase (FAAH) to treat pain and inflammation. *AAPS J.* 2009; 11 (1):39–44. [PubMed: 19184452]
13. Kathuria S, et al. Modulation of anxiety through blockade of anandamide hydrolysis. *Nat Med.* 2003; 9 (1):76–81. [PubMed: 12461523]
14. Piomelli D, et al. Pharmacological profile of the selective FAAH inhibitor KDS-4103 (URB597). *CNS Drug Rev.* 2006; 12 (1):21–38. [PubMed: 16834756]
15. Clapper JR, et al. A second generation of carbamate-based fatty acid amide hydrolase inhibitors with improved activity in vivo. *ChemMedChem.* 2009; 4 (9):1505–1513. [PubMed: 19637155]
16. Alexander JP, Cravatt BF. Mechanism of carbamate inactivation of FAAH: implications for the design of covalent inhibitors and in vivo functional probes for enzymes. *Chem Biol.* 2005; 12 (11):1179–1187. [PubMed: 16298297]
17. Loscher W, Potschka H. Blood-brain barrier active efflux transporters: ATP-binding cassette gene family. *NeuroRx.* 2005; 2 (1):86–98. [PubMed: 15717060]
18. Mulder GJ, Scholtens E. Phenol sulphotransferase and uridine diphosphate glucuronyltransferase from rat liver in vivo and vitro. 2,6-Dichloro-4-nitrophenol as selective inhibitor of sulphation. *Biochem J.* 1977; 165 (3):553–559. [PubMed: 411489]
19. Imai Y, et al. Breast cancer resistance protein exports sulfated estrogens but not free estrogens. *Mol Pharmacol.* 2003; 64 (3):610–618. [PubMed: 12920197]
20. LoVerme J, La Rana G, Russo R, Calignano A, Piomelli D. The search for the palmitoylethanolamide receptor. *Life Sci.* 2005; 77 (14):1685–1698. [PubMed: 15963531]
21. Cravatt BF, et al. Supersensitivity to anandamide and enhanced endogenous cannabinoid signaling in mice lacking fatty acid amide hydrolase. *Proc Natl Acad Sci U S A.* 2001; 98 (16):9371–9376. [PubMed: 11470906]
22. Starowicz K, Nigam S, Di Marzo V. Biochemistry and pharmacology of endovanilloids. *Pharmacol Ther.* 2007; 114 (1):13–33. [PubMed: 17349697]
23. LoVerme J, et al. Rapid broad-spectrum analgesia through activation of peroxisome proliferator-activated receptor- α . *J Pharmacol Exp Ther.* 2006; 319 (3):1051–1061. [PubMed: 16997973]
24. Russo R, et al. Synergistic antinociception by the cannabinoid receptor agonist anandamide and the PPAR- α receptor agonist GW7647. *Eur J Pharmacol.* 2007; 566 (1–3):117–119. [PubMed: 17434479]
25. Bennett GJ, Xie YK. A peripheral mononeuropathy in rat that produces disorders of pain sensation like those seen in man. *Pain.* 1988; 33 (1):87–107. [PubMed: 2837713]
26. Russo R, et al. The fatty acid amide hydrolase inhibitor URB597 (cyclohexylcarbamic acid 3'-carbamoylbiphenyl-3-yl ester) reduces neuropathic pain after oral administration in mice. *J Pharmacol Exp Ther.* 2007; 322 (1):236–242. [PubMed: 17412883]
- 27.Coderre TJ, Melzack R. The contribution of excitatory amino acids to central sensitization and persistent nociception after formalin-induced tissue injury. *J Neurosci.* 1992; 12 (9):3665–3670. [PubMed: 1326610]
28. Puig S, Sorkin LS. Formalin-evoked activity in identified primary afferent fibers: systemic lidocaine suppresses phase-2 activity. *Pain.* 1996; 64 (2):345–355. [PubMed: 8740613]
29. Kunos G, Osei-Hyiaman D, Batkai S, Sharkey KA, Makriyannis A. Should peripheral CB(1) cannabinoid receptors be selectively targeted for therapeutic gain? *Trends Pharmacol Sci.* 2009; 30 (1):1–7. [PubMed: 19042036]

30. Ahluwalia J, Yaqoob M, Urban L, Bevan S, Nagy I. Activation of capsaicin-sensitive primary sensory neurones induces anandamide production and release. *J Neurochem.* 2003; 84 (3):585–591. [PubMed: 12558978]
31. Liu J, et al. A biosynthetic pathway for anandamide. *Proc Natl Acad Sci U S A.* 2006; 103 (36): 13345–13350. [PubMed: 16938887]
32. Hohmann AG, Herkenham M. Localization of central cannabinoid CB1 receptor messenger RNA in neuronal subpopulations of rat dorsal root ganglia: a double-label in situ hybridization study. *Neuroscience.* 1999; 90 (3):923–931. [PubMed: 10218792]
33. Hohmann AG, Herkenham M. Cannabinoid receptors undergo axonal flow in sensory nerves. *Neuroscience.* 1999; 92 (4):1171–1175. [PubMed: 10426476]
34. Richardson JD, Kilo S, Hargreaves KM. Cannabinoids reduce hyperalgesia and inflammation via interaction with peripheral CB1 receptors. *Pain.* 1998; 75 (1):111–119. [PubMed: 9539680]
35. Guindon J, Hohmann AG. Cannabinoid CB2 receptors: a therapeutic target for the treatment of inflammatory and neuropathic pain. *Br J Pharmacol.* 2008; 153 (2):319–334. [PubMed: 17994113]
36. Sagar DR, Kendall DA, Chapman V. Inhibition of fatty acid amide hydrolase produces PPAR-alpha-mediated analgesia in a rat model of inflammatory pain. *Br J Pharmacol.* 2008; 155 (8): 1297–1306. [PubMed: 18724387]
37. Cravatt BF, et al. Functional disassociation of the central and peripheral fatty acid amide signaling systems. *Proc Natl Acad Sci U S A.* 2004; 101 (29):10821–10826. [PubMed: 15247426]
38. Lever IJ, et al. Localization of the endocannabinoid-degrading enzyme fatty acid amide hydrolase in rat dorsal root ganglion cells and its regulation after peripheral nerve injury. *J Neurosci.* 2009; 29 (12):3766–3780. [PubMed: 19321773]
39. Tegeder I, et al. Peripheral opioid analgesia in experimental human pain models. *Brain.* 2003; 126 (Pt 5):1092–1102. [PubMed: 12690049]
40. Mor M, et al. Cyclohexylcarbamic acid 3'- or 4'-substituted biphenyl-3-yl esters as fatty acid amide hydrolase inhibitors: synthesis, quantitative structure-activity relationships, and molecular modeling studies. *J Med Chem.* 2004; 47 (21):4998–5008. [PubMed: 15456244]
41. King AR, et al. URB602 inhibits monoacylglycerol lipase and selectively blocks 2-arachidonoylglycerol degradation in intact brain slices. *Chem Biol.* 2007; 14 (12):1357–1365. [PubMed: 18096504]
42. Astarita G, Ahmed F, Piomelli D. Identification of biosynthetic precursors for the endocannabinoid anandamide in the rat brain. *J Lipid Res.* 2008; 49 (1):48–57. [PubMed: 17957091]
43. Calignano A, La Rana G, Piomelli D. Antinociceptive activity of the endogenous fatty acid amide, palmitylethanolamide. *Eur J Pharmacol.* 2001; 419 (2–3):191–198. [PubMed: 11426841]
44. Tjolsen A, Berge OG, Hunskaar S, Rosland JH, Hole K. The formalin test: an evaluation of the method. *Pain.* 1992; 51 (1):5–17. [PubMed: 1454405]
45. Fegley D, et al. Characterization of the fatty acid amide hydrolase inhibitor cyclohexyl carbamic acid 3'-carbamoyl-biphenyl-3-yl ester (URB597): effects on anandamide and oleoylethanolamide deactivation. *J Pharmacol Exp Ther.* 2005; 313 (1):352–358. [PubMed: 15579492]
46. Cadas H, di Tomaso E, Piomelli D. Occurrence and biosynthesis of endogenous cannabinoid precursor, N-arachidonoyl phosphatidylethanolamine, in rat brain. *J Neurosci.* 1997; 17 (4):1226–1242. [PubMed: 9006968]
47. Presley RW, Menetrey D, Levine JD, Basbaum AI. Systemic morphine suppresses noxious stimulus-evoked Fos protein-like immunoreactivity in the rat spinal cord. *J Neurosci.* 1990; 10 (1): 323–335. [PubMed: 1688935]
48. Paxinos, G.; Watson, C. *The rat brain in stereotaxic coordinates.* 6. Academic Press/Elsevier; Amsterdam ; Boston : 2007.
49. Eddy NB, Leimbach D. Synthetic analgesics. II. Dithienylbutenyl- and dithienylbutylamines. *J Pharmacol Exp Ther.* 1953; 107 (3):385–393. [PubMed: 13035677]
50. Ruda MA, Ling QD, Hohmann AG, Peng YB, Tachibana T. Altered nociceptive neuronal circuits after neonatal peripheral inflammation. *Science.* 2000; 289 (5479):628–631. [PubMed: 10915627]
51. Hargreaves K, Dubner R, Brown F, Flores C, Joris J. A new and sensitive method for measuring thermal nociception in cutaneous hyperalgesia. *Pain.* 1988; 32 (1):77–88. [PubMed: 3340425]

52. Gaetani S, Oveisi F, Piomelli D. Modulation of meal pattern in the rat by the anorexic lipid mediator oleoylethanolamide. *Neuropsychopharmacology*. 2003; 28 (7):1311–1316. [PubMed: 12700681]

**Figure 1.**

URB937 is a peripherally restricted FAAH inhibitor. **(a)** FAAH activity in liver (closed circles) and brain (closed squares) 1 h after injection of URB937 (0.03–100 mg·kg⁻¹, s.c.) in Swiss Webster mice. **(b)** Temporal distribution of URB937 in liver, brain and serum (inset) after a single injection in Swiss-webster mice (1 mg·kg⁻¹, i.p.). **(c)** Serum concentrations of URB937 after i.c.v. infusion in rats (0.01–0.1 mg·kg⁻¹). **(d)** Liver FAAH activity after intracerebroventricular (i.c.v.) infusion of vehicle (open bar) or URB937 (0.01–0.1 mg·kg⁻¹, closed bars) in rats. **(e)** Brain FAAH activity after systemic administration of vehicle (V), URB597 (1 mg·kg⁻¹, s.c.), or URB937 (shaded bar: 1 mg·kg⁻¹; closed bars: 25 mg·kg⁻¹, s.c.); URB937 was administered alone or in combination with drug-transport inhibitors, 2,6-dichloro-4-nitrophenol (DCNP, 40 mg·kg⁻¹, i.p.), Ko-143 (Ko, 10 mg·kg⁻¹, i.p.), verapamil (Ver, 50 mg·kg⁻¹, i.p.), probenecid (Pro, 150 mg·kg⁻¹, i.p.), and rifampicin (Rif, 50 mg·kg⁻¹, i.p.). **(f)** Effects of vehicle (open bars) or URB937 (1 mg·kg⁻¹, i.p., closed bars) on anandamide and palmitoylethanolamide (PEA) levels in liver, forebrain and hypothalamus of Swiss Webster mice. **(g)** Effects of URB937 on anandamide and PEA levels in liver of wild-type C57Bl/6 mice (+/+) and FAAH-deficient littermates (-/-). Results are expressed as mean ± s.e.m; *n* = 3; **P* < 0.05 and ****P* < 0.001 vs vehicle.

**Figure 2.**

URB937 suppresses pain responses elicited by i.p. injections of acetic acid in Swiss Webster mice. **(a)** Behavioral score (number of writhing episodes in 20 min) assessed 1 h after administration of vehicle (V, open bars), URB937, URB597, or indomethacin (IDM) (each at $1 \text{ mg}\cdot\text{kg}^{-1}$, s.c., closed bars). Also illustrated are the effects of vehicle and URB937 administered without acetic acid. **(b)** Statistical correlation between behavioral score and percent inhibition of liver FAAH activity after URB937 administration ($1 \text{ mg}\cdot\text{kg}^{-1}$, s.c.). **(c)** Effects of vehicle (open bars) or URB937 ($1 \text{ mg}\cdot\text{kg}^{-1}$, s.c., closed bars) on acetic acid-induced writhing in wild-type C57Bl/6 mice (+/+) and FAAH-deficient littermates (-/-). **(d)** CB₁ antagonists rimonabant (Rim) and AM251, and PPAR- α antagonist MK886 (each at $1 \text{ mg}\cdot\text{kg}^{-1}$, s.c.) prevent the antinociceptive effects of URB937. CB₂ antagonist AM630 is ineffective. **(e)** Effects of vehicle (open bars) or URB937 ($1 \text{ mg}\cdot\text{kg}^{-1}$, s.c., closed bars) on acetic acid-induced writhing in wild-type C57Bl/6 mice (+/+) and PPAR- α -deficient mice (-/-). Results are expressed as mean \pm s.e.m.; $n = 5\text{--}17$. * $P < 0.05$; ** $P < 0.01$ and *** $P < 0.001$ vs vehicle.

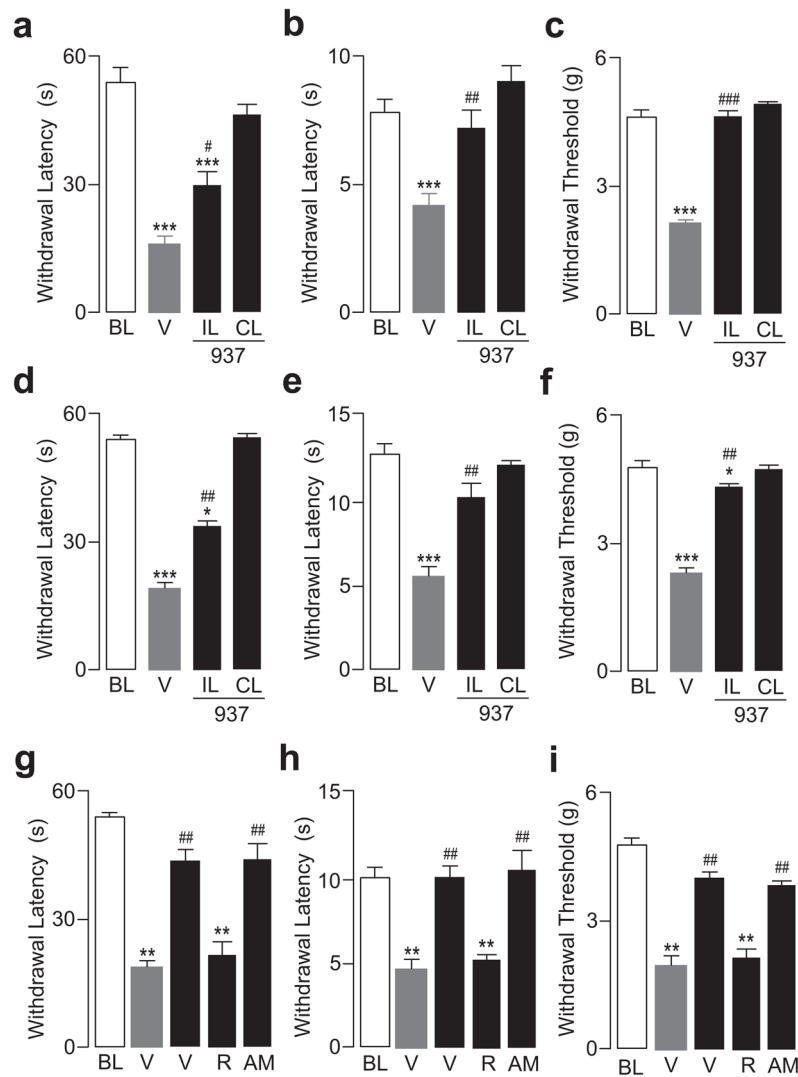
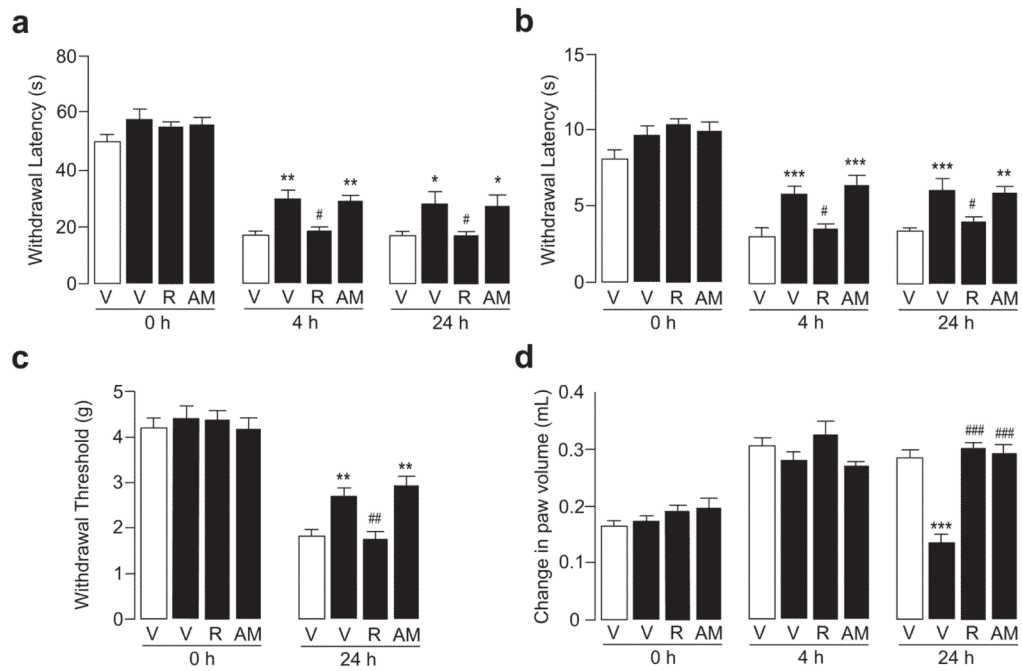


Figure 3.

URB937 suppresses pain behavior elicited by neural injury in mice. **(a-c)** Effects of single administration of vehicle (shaded bars) or URB937 ($1 \text{ mg}\cdot\text{kg}^{-1}$, i.p.; closed bars) on **(a)** mechanical hyperalgesia, **(b)** thermal hyperalgesia, and **(c)** mechanical allodynia produced by sciatic nerve ligation. BL, baseline (measured before nerve ligation); IL, ipsilateral (ligated) paw; CL, contralateral (non-ligated) paw. **(d-f)** Effects of repeated injections of vehicle or URB937 ($1 \text{ mg}\cdot\text{kg}^{-1}$, i.p., once-daily for 7 consecutive days) on **(d)** mechanical hyperalgesia, **(e)** thermal hyperalgesia, and **(f)** mechanical allodynia. **(g-i)** CB_1 antagonist rimonabant (R, $1 \text{ mg}\cdot\text{kg}^{-1}$, i.p.), but not CB_2 antagonist AM630 (AM, $1 \text{ mg}\cdot\text{kg}^{-1}$, i.p.), prevents the effects of URB937 on **(g)** mechanical hyperalgesia, **(h)** thermal hyperalgesia, and **(i)** mechanical allodynia. Results are expressed as mean \pm s.e.m.; $n = 6$ in each panel. * $P < 0.05$, ** $P < 0.01$ and *** $P < 0.001$ vs baseline; # $P < 0.05$, ## $P < 0.01$ and ### $P < 0.001$ vs vehicle.

**Figure 4.**

URB937 attenuates pain behavior elicited by inflammation in mice. Effects of URB937 ($1 \text{ mg}\cdot\text{kg}^{-1}$, i.p.), administered alone or in combination with rimonabant (R, $1 \text{ mg}\cdot\text{kg}^{-1}$, i.p.) or AM630 (AM, $1 \text{ mg}\cdot\text{kg}^{-1}$, i.p.), on carrageenan-induced responses: (a) mechanical hyperalgesia; (b) thermal hyperalgesia; (c) mechanical allodynia; and (d) paw edema. Mechanical and thermal hyperalgesia were measured immediately before carrageenan injection (0 h) or 4 h and 24 h after injection. Mechanical allodynia was measured 0 h and 24 h after carrageenan. Results are expressed as mean \pm s.e.m.; $n = 6$. * $P < 0.05$, ** $P < 0.01$ and *** $P < 0.001$ vs vehicle; # $P < 0.05$, ## $P < 0.01$ and ### $P < 0.001$ vs URB937.

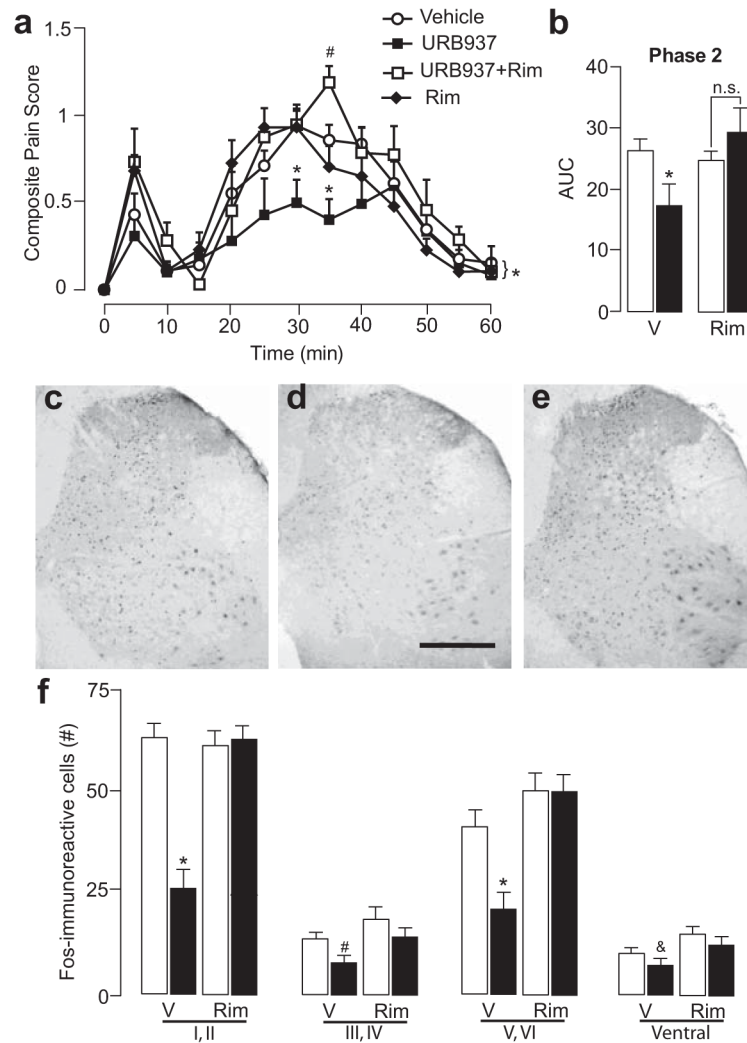
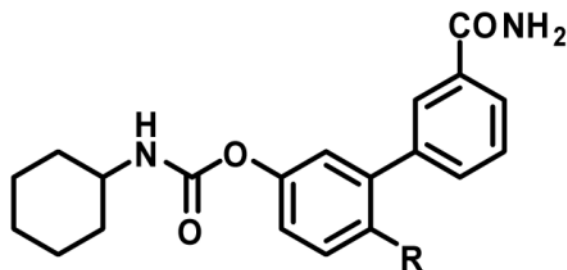


Figure 5. URB937 attenuates formalin-induced pain behavior and spinal cord Fos protein expression in rats. (a) URB937 ($1 \text{ mg}\cdot\text{kg}^{-1}$, i.p.), injected together with formalin, produced time-dependent changes in composite pain score relative to vehicle, rimonabant (Rim, $2 \text{ mg}\cdot\text{kg}^{-1}$, i.p.) or a combination of URB937 and rimonabant ($F_{14,22} = 1.86$, $P = 0.039$). (b) URB937 decreased area under the curve (AUC) of pain behavior during Phase 2 of the formalin response (10–60 min; $F_{1,3} = 3.05$, $P = 0.050$). Results are expressed as mean \pm s.e.m.; $n = 5-7$. * $P < 0.05$, all groups vs URB937; # $P < 0.05$, URB937 plus rimonabant vs vehicle. (c–e) Representative sections of lumbar spinal cord showing formalin-induced Fos-positive cells after injection of (c) vehicle; (d) URB937 ($1 \text{ mg}\cdot\text{kg}^{-1}$, i.p.); or (e) URB937 plus rimonabant ($2 \text{ mg}\cdot\text{kg}^{-1}$, i.p.). Calibration bar, 0.5 mm. (f) Quantitative analysis of the effects of vehicle (open bars), URB937 (closed bars), rimonabant (Rim), and URB937 plus rimonabant on number of Fos-positive cells in superficial dorsal horn (lamina I, II), nucleus proprius (lamina III, IV), neck region of the dorsal horn (lamina V, VI), and ventral horn. Results are expressed as mean \pm s.e.m.; $n = 5-7$. * $P < 0.05$, all groups vs URB937; # $P < 0.05$, URB937 plus rimonabant, or rimonabant alone vs URB937; & $P < 0.05$, vehicle, or rimonabant alone vs URB937.

Table 1

In vitro and *in vivo* characterization of *O*-arylcarbamate FAAH inhibitors

Compound	R	IC ₅₀ (nM) ^a	FAAH Inhibition in liver (%) ^b	FAAH Inhibition in brain (%) ^b
1a (URB597)	H	7.7 ± 1.5	Not determined	96.2 ± 0.4
1b (URB937)	OH	26.8 ± 4.9	91.7 ± 0.7	-3.0 ± 8.0
1c	OCH ₃	45.3 ± 14.1	94.6 ± 0.7	86.4 ± 2.1
1d	CH ₃	20.5 ± 0.6	93.0 ± 1.1	91.9 ± 1.5
1e	F	49.7 ± 5.8	90.7 ± 1.2	89.7 ± 1.3
1f	NH ₂	42.5 ± 4.2	92.2 ± 0.6	23.2 ± 2.1

^aIC₅₀ measured in membrane preparations of Wistar rat brain^bFAAH inhibition measured *ex vivo* 1 h after injection in Swiss Webster mice (1 mg·kg⁻¹, i.p., n = 3)